EHD2 regulates adipocyte function and is enriched at cell surface–associated lipid droplets in primary human adipocytes

Björn Morén[a], Björn Hansson[a], Florentina Negoita[a], Claes Fryklund[a], Richard Lundmark[b], Olga Göransson[a], and Karin G. Stenkula[a,*]

[a]Department of Experimental Medical Science, Lund University, 223 84 Lund, Sweden; [b]Medical Biochemistry and Biophysics, Umeå University, 901 87 Umeå, Sweden

ABSTRACT **Adipocytes play a central role in energy balance, and dysfunctional adipose tissue severely affects systemic energy homeostasis. The ATPase EH domain–containing 2 (EHD2) has previously been shown to regulate caveolae, plasma membrane-specific domains that are involved in lipid uptake and signal transduction. Here, we investigated the role of EHD2 in adipocyte function. We demonstrate that EHD2 protein expression is highly up-regulated at the onset of triglyceride accumulation during adipocyte differentiation. Small interfering RNA–mediated EHD2 silencing affected the differentiation process and impaired insulin sensitivity, lipid storage capacity, and lipolysis. Fluorescence imaging revealed localization of EHD2 to caveolae, close to cell surface–associated lipid droplets in primary human adipocytes. These lipid droplets stained positive for glycerol transporter aquaporin 7 and phosphorylated perilipin-1 following adrenergic stimulation. Further, EHD2 overexpression in human adipocytes increased the lipolytic signaling and suppressed the activity of transcription factor PPARγ. Overall, these data suggest that EHD2 plays a key role for adipocyte function.**

Monitoring Editor
Jean E. Gruenberg
University of Geneva

Received: Oct 25, 2018
Revised: Feb 20, 2019
Accepted: Feb 22, 2019

INTRODUCTION

Adipose tissue constitutes the main storage site of excess energy in the form of triglycerides that are released as free fatty acids (FFA) when needed. Impaired energy storage capacity in adipocytes is associated with increased levels of circulating FFA and with ectopic lipid accumulation in liver and muscle, which is a major risk factor for developing insulin resistance and type 2 diabetes (Schinner *et al.*, 2005). We and others have examined the dynamics of adipose tissue expansion (McLaughlin *et al.*, 2007; Li *et al.*, 2016; Hansson *et al.*, 2018), which involves increased adipocyte size (hypertrophy) as well as increased cell number (hyperplasia). The latter occurs through differentiation of preadipocytes (adipogenesis) (Salans *et al.*, 1968), a process tightly regulated by various transcription factors, including peroxisome proliferator-activated receptor gamma (PPARγ) and CCAAT/enhancer-binding proteins alpha and beta (C/EBPα and C/EBPβ). Recent studies have implicated impaired differentiation (Grunberg *et al.*, 2014; Acosta *et al.*, 2016) and limited adipocyte expansion (McLaughlin *et al.*, 2007, 2014) as factors contributing to adipose tissue dysfunction and a worsened systemic metabolic profile.

Recently, we identified EH domain–containing 2 (EHD2) as one of the most highly up-regulated genes in adipose tissue during short-term overfeeding in mice (Hansson *et al.*, 2018). EHD2 belongs to a family of well-conserved dynamin-related ATPase proteins (EHD1–4) that are implicated in several cellular processes, including membrane recycling, receptor internalization, and GLUT4 endocytosis (Guilherme *et al.*, 2004; Naslavsky *et al.*, 2004; Park *et al.*, 2004). The ability of EHD proteins to form ring-like oligomers on lipid membranes, thereby causing membrane curvature, has

This article was published online ahead of print in MBoC in Press (http://www.molbiolcell.org/cgi/doi/10.1091/mbc.E18-10-0680) on February 27, 2019.

*Address correspondence to: Karin Stenkula (Karin.stenkula@med.lu.se).

No competing interests declared.

Abbreviations used: ACC, acetyl-CoA carboxylase; AQP7, aquaporin 7; ATGL, adipose triglyceride lipase; AU, arbitrary units; BSA, bovine serum albumin; C/EBPα, CCAAT/enhancer-binding protein alpha; C/EBPβ, CCAAT/enhancer-binding protein beta; EHD2, EH domain–containing 2; FAS, fatty acid synthase; FCS, fetal calf serum; FFA, free fatty acids; FIRKO, adipose tissue-specific insulin receptor knockout; HFD, high-fat diet; HSL, hormone-sensitive lipase; HSP, heat shock protein; ISO, isoprenaline; KO, knockout; KRBH, Krebs-Ringer Bicarbonate HEPES; mLD, microlipid droplets; PIA, phenyl-isopropyl-adenosin; PPARγ, peroxisome proliferator-activated receptor gamma; PPRE, PPAR response element; SCR, siRNA control; siEHD2, EHD2 siRNA; SREBP1c, sterol regulatory element-binding protein 1c; WT, wild type.

highlighted their role in membrane trafficking (Daumke *et al.*, 2007). Mass spectrometry and vectorial proteomics revealed EHD2 to be associated with caveolae (Aboulaich *et al.*, 2004), specific invaginations of the plasma membrane that are implicated in numerous processes, including signal transduction (Gustavsson *et al.*, 1999), cholesterol efflux (Fielding and Fielding, 2001), and lipid transport (Meshulam *et al.*, 2006; Ding *et al.*, 2014). Indeed, ablation or mutation of the caveolar core protein caveolin-1 causes impaired insulin signaling in mice (Cohen *et al.*, 2003) and lipodystrophy in humans (Kim *et al.*, 2008). The past decade, a central role of cavin proteins for caveolae assembling and function has emerged (Bastiani *et al.*, 2009; Parton and del Pozo, 2013; Kovtun *et al.*, 2015). Studies at the ultrastructural level, in nonadipocyte cell models, have demonstrated that EHD2 is located specifically at the neck of caveolae (Moren *et al.*, 2012; Ludwig et al., 2013; Shah *et al.*, 2014). Based on previous knowledge of EHD2 function related to its ATPase activity (Daumke *et al.*, 2007), it was hypothesized that EHD2, by constraining the caveolar neck, would regulate the stability, but not the formation, of caveolae at the plasma membrane (Moren *et al.*, 2012). This assumption was confirmed by the finding that EHD2 knockdown lead to increased caveolae mobility, whereas EHD2 overexpression immobilized caveolae and prolonged the duration of their localization to the plasma membrane surface (Moren *et al.*, 2012; Stoeber *et al.*, 2012). Caveolin-1, together with EHD2, has also been shown to associate with intracellular lipid droplets by mass spectrometry (Blouin *et al.*, 2010). Caveolae are also considered a membrane reservoir, and EHD2 was recently reported to serve as a mechanosensor connecting caveolae with transcriptional activity (Torrino *et al.*, 2018). Few studies have addressed the biological function of EHD2 in adipocyte biology.

Here, we demonstrate that EHD2 is up-regulated in parallel with caveolin-1 during adipocyte differentiation. Further, we discovered EHD2 to be located, together with caveolin-1, in close proximity of cell surface-associated lipid droplets that displayed lipolytic activity in fully differentiated human adipocytes. Together, these data suggest that EHD2 plays a key role in maintaining adipocyte function and lipid metabolism, possibly indirectly by affecting caveolae function.

RESULTS

Increased expression of EHD2 and caveolin-1 in adipose tissue following high-fat diet

First, we examined the relationship between caveolin-1 and EHD2 expression in adipose tissue using RNA sequence data previously obtained from adipose tissue during a short-term (14 d) overfeeding study in mice (Hansson *et al.*, 2018). By analyzing that data set, we found a positive correlation between EHD2 and caveolin-1 mRNA expression (Figure 1A). Western blot analysis demonstrated that the protein levels of caveolin-1 and EHD2 had increased three- and two-fold, respectively, after 14 d of high-fat diet (HFD) (Figure 1B). While the protein level of caveolin-1 rapidly increased after 2 d, the EHD2 level increased after 14 d, a time point that we previously (Hansson *et al.*, 2018) demonstrated to coincide with considerable adipocyte differentiation. Next, by comparing the EHD2 levels in adipose tissue versus isolated adipocytes from chow- or HFD-fed mice, we found that the increase of EHD2 in adipose tissue following HFD was not due to an increase in the isolated adipocytes (Figure 1C). We interpret the increased EHD2 levels to reflect an increased adipocyte differentiation and, hence, an increased proportion of mature adipocytes within the tissue. Further, we found EHD2 to be completely down-regulated in tissues from caveolin-1–deficient mice, a mouse model known to have severe lipodystrophy (Figure 1D). Together these data imply that EHD2 expression is tightly related to expression of caveolin-1.

EHD2 is up-regulated during adipocyte maturation

Since EHD2 seemed to be significantly up-regulated at a stage of pronounced adipocyte differentiation, we investigated the expression and subcellular localization of EHD2 during adipocyte maturation using cultured 3T3-L1 cells. Four days after initiating differentiation (initiation at day 0), a distinct increase of EHD2 protein expression coincided with increased expression of caveolin-1 and fatty acid synthase (FAS) (Figure 1E). C/EBPα expression was monitored to verify adipocyte maturation (Figure 1E). At the same time point (day 4), confocal microscopy demonstrated a clear accumulation of intracellular lipid droplets (Figure 1, F and G, top panels). As expected, larger intracellular lipid droplets were formed at the later stages of differentiation (day 11). The localization of EHD2 and caveolin-1 gradually shifted from striated patterns (day –2) to distinct structures (day 11) at the membrane surface, which most likely reflect plasma membrane-associated caveolae (EHD2 and caveolin-1 shown in bottom panels in Figure 1, F and G, respectively). Higher temporal resolution of the lipid droplet accumulation and redistribution of EHD2 and caveolin-1 during differentiation is shown in Supplemental Figure S1. Colabeling against EHD2 and caveolin-1 at a later stage of differentiation (day 11) demonstrated that EHD2 and caveolin-1 localized to the same structures (Figure 1H). Colabeling against EHD2 and cavin1, another caveolae-related protein, displayed a similar pattern (Supplemental Figure S2A). Thus, EHD2 expression seems to follow the formation of caveolae structures during adipocyte maturation.

EHD2 silencing halts adipocyte maturation

To further examine the role of EHD2 in adipocyte function, we employed small interfering RNA (siRNA)-mediated gene silencing of EHD2 in 3T3-L1 cells 4 d after initiating the differentiation. After 72 h, the EHD2 mRNA level was significantly suppressed (data not shown), and Western blot analysis confirmed a complete knockdown of EHD2 at the protein level (Figure 2, A and B). EHD2 silencing was associated with reduced levels of PPARγ2, CEBPα, and adiponectin, the latter an adipocyte-specific hormone, which promotes adipocyte differentiation (Fu *et al.*, 2005) (Figure 2, A and B). The protein level of C/EBPβ was unchanged. Further, EHD2 silencing reduced the expression of proteins involved in lipid metabolism; acetyl-CoA carboxylase (ACC), FAS, sterol regulatory element-binding protein 1c (SREBP1c), and perilipin-1, whereas adipose triglyceride lipase (ATGL), ap2 (a carrier protein for fatty acids), caveolin-1, and cavin1 were similar compared with control (Figure 2, C and D). Consistent with the down-regulation of proteins involved in de novo lipid synthesis and lipid metabolism, the total lipid accumulation in EHD2-silenced cells was decreased, as assessed by confocal microscopy (Figure 3, A and B). Image analysis also revealed an accumulation of smaller lipid droplets in EHD2-silenced cells compared with control cells (Figure 3C). EHD2 silencing did not affect the distribution of caveolin-1 (Figure 3D), which is in line with previous reports (Moren *et al.*, 2012). The decreased levels of PPARγ2, CEBPα, and SREBP1c suggest that knockdown of EHD2 alters the differentiation process, which could, at least partially, explain the decreased expression of proteins involved in lipid metabolism and also the impaired lipid storage.

Impaired hormonal response in EHD2-silenced cells

Sensitivity to the metabolic hormones insulin and catecholamine is a key feature of normal adipocyte function. To explore whether

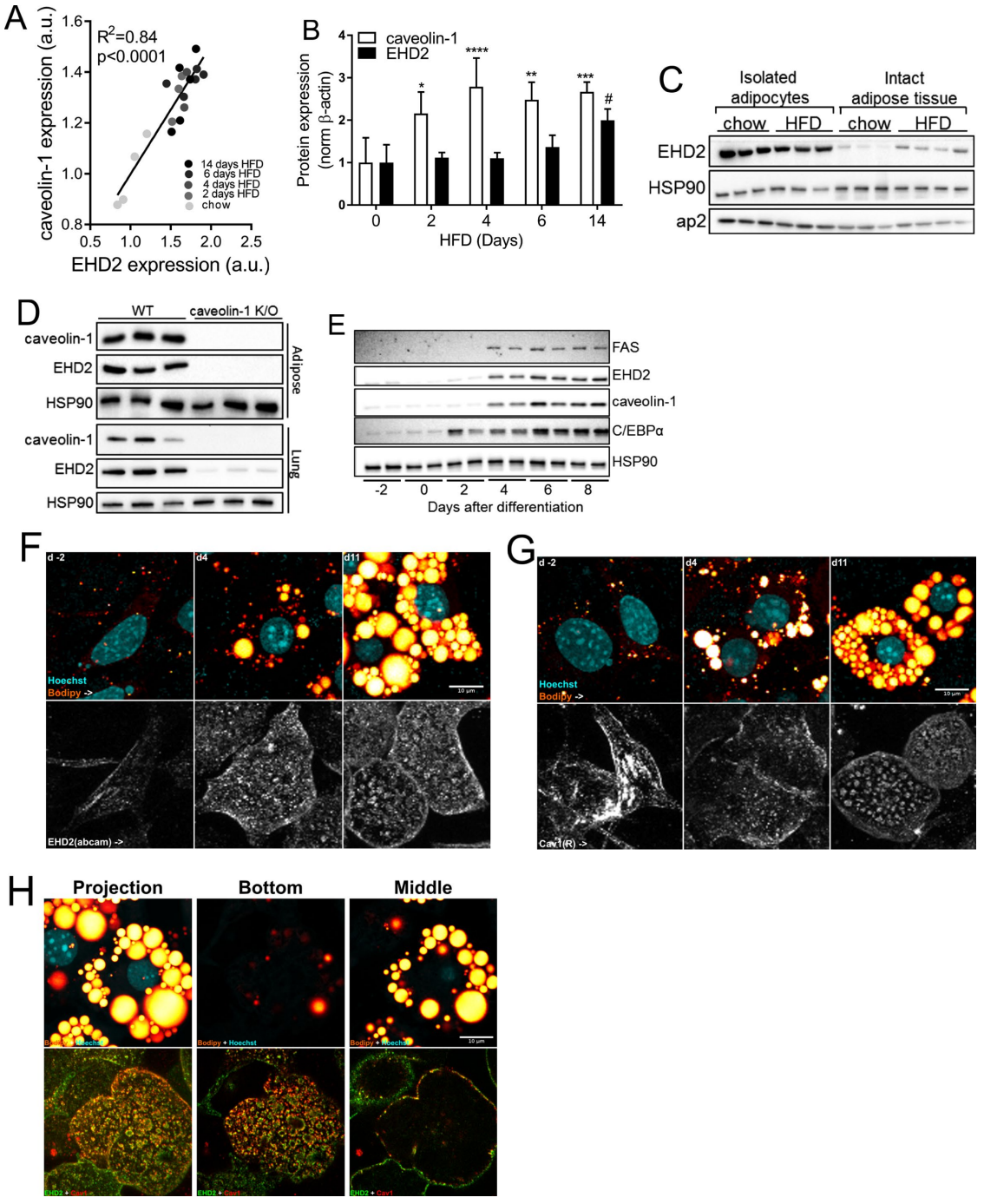

FIGURE 1: (A) Correlation between EHD2 and caveolin-1 mRNA expression in epididymal fat tissue during 14 d of HFD feeding of C57BL6/J mice, $n = 20$ biological data points. (B) Protein expression of EHD2 and caveolin-1 in epididymal adipose tissue during 14 d of HFD, $n = 3$–4/group, data normalized to β-actin. (C) Western blot analysis showing EHD2 protein expression in isolated primary adipocytes and epididymal adipose tissue from mice fed chow or 14 d of HFD, HSP90 used as a loading control, ap2 used as an adipocyte marker. (D) Western blot analysis showing caveolin-1 and EHD2 protein expression in epididymal adipose and lung tissues from WT- and caveolin-1 KO mice. $n = 3$ animals/group; HSP90 used as a loading control. (E) Representative blots showing protein expression of FAS, EDH2, caveolin-1, and C/EBPα during 3T3-L1 differentiation, $n = 4$ independent experiments; each sample was collected and is presented as a technical duplicate. HSP90 used as a loading control. (F) Representative immunofluorescence microscopy images of differentiating 3T3-L1 cells –2, 4, and 11 d after initiating differentiation. Cells were stained with Hoechst (blue signal, nuclei), BODIPY (yellow signal, neutral lipids) (top panel), and EHD2 antibody (bottom panel). (G) Same as in F but stained for caveolin-1 instead of EHD2 (caveolin-1 shown in bottom panel, Cav1). (H) Representative images showing a projection, bottom and middle sections of 3T3-L1 cells, 8 d after differentiation, costained with direct-conjugated antibodies toward EHD2 and caveolin-1, Hoechst, and BODIPY. Data in B are presented as mean ± SD. #,*$p < 0.05$, **$p < 0.01$, ***$p < 0.001$, and ****$p < 0.0001$ represent significance compared with 0 d of HFD. Scale bar = 10 μm.

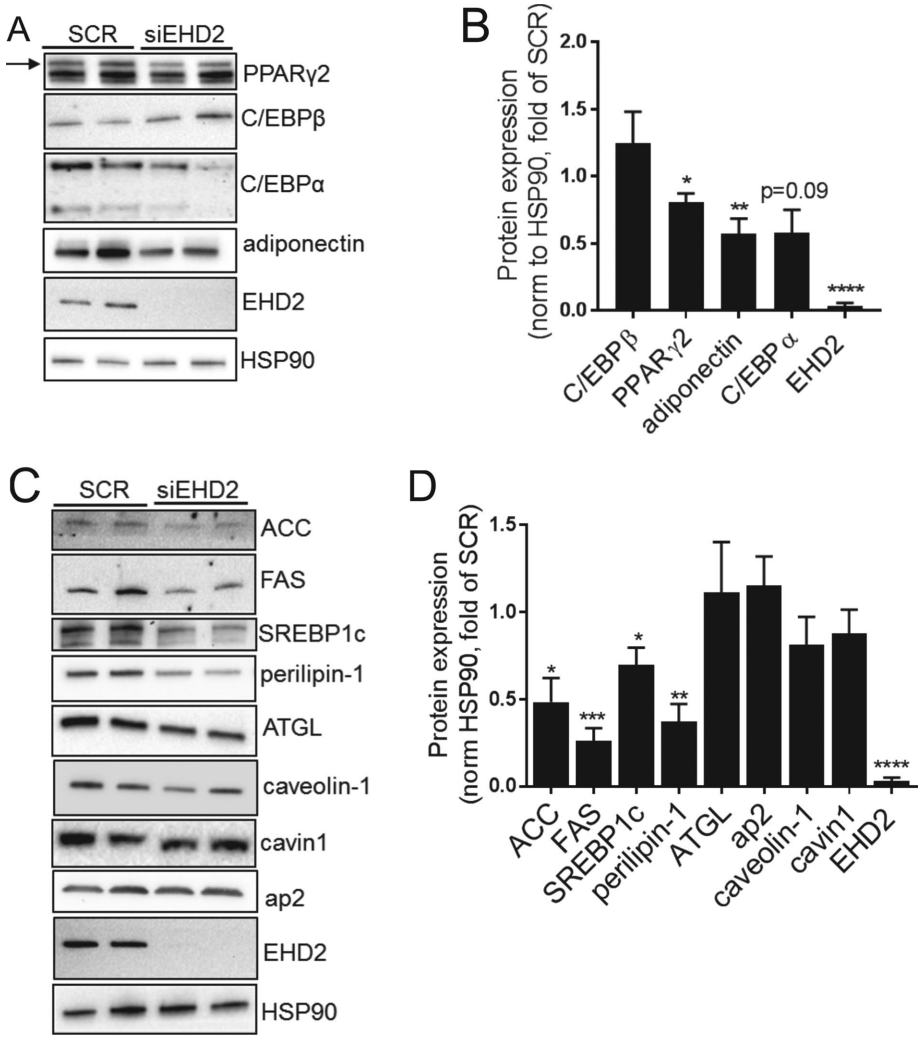

FIGURE 2: (A) Representative Western blots of EHD2 and transcriptional targets in 3T3-L1 cell lysates collected 72 h after gene silencing with siRNA control (SCR) or EHD2 siRNA (siEHD2). HSP90 was used as a loading control. Arrow indicates PPARγ2. (B) Quantification of protein expression in A normalized to HSP90. $n = 4$ independent experiments; each sample was collected and presented as a technical duplicate. (C) Representative Western blots of targets involved in lipid metabolism in 3T3-L1 cell lysates were collected 72 h after gene silencing with siRNA control (SCR) or siEHD2. HSP90 was used as a loading control. (D) Quantification of protein expression in C normalized to HSP90. $n = 4$ independent experiments; each experiment was run in duplicate. Data are presented as mean ± SD. *$p < 0.05$, **$p < 0.01$, ***$p < 0.001$, and ****$p < 0.0001$.

EHD2 silencing also affected the insulin response, scrambled or EHD2-silenced cells were stimulated with a submaximal or maximal dose of insulin (0.01 and 10 nM, respectively) 72 h after gene silencing. Western blot analysis demonstrated that insulin-stimulated phosphorylation of IRS-1 Y612, PKB S473, and T308 (bottom panel), and the total IRS-1 level, were all reduced in EHD2-silenced cells, whereas the total PKB level seemed unchanged (Figure 4A; quantifications are shown in Figure 4B). Further, EHD2 silencing also suppressed both basal and catecholamine-induced (isoprenaline [ISO], 10 and 100 nM) glycerol release (Figure 4C). Note that the glycerol release was still lower in EHD2-silenced cells even if normalized to the initial triglyceride content (Supplemental Figure S2B). In line with this, total and phosphorylated levels of perilipin-1 (S522), the latter used to detect cAMP-dependent lipolysis, and hormone-sensitive lipase (HSL) at site S563 were markedly reduced (Figure 4D). Quantification demonstrated that the fold response of HSL pS563 following catecholamine stimulation was decreased in EHD2-silenced cells compared with control (Figure 4E). Further, immunofluorescence microscopy revealed a marked increase in perilipin-1 pS522 stain after ISO incubation in control, but not in EHD2-silenced cells (Figure 4F, left panels: unstimulated condition [CTRL]; right panels: ISO-stimulated condition; perilipin-1 pS522 shown in red). Thus, EHD2 silencing decreased the expression and hormonal response of proteins involved in insulin signal transduction and hydrolysis of triglycerides.

Localization of EHD2 to caveolae in primary human adipocytes

So far, our data suggest that EHD2 is upregulated during adipocyte maturation and is required to maintain intact adipocyte function. Since EHD2 has been reported to regulate caveolae stability in nonadipocyte cell lines (Moren *et al.*, 2012), and caveolae are key for maintained lipid storage function and insulin signal transduction in adipocytes (Razani *et al.*, 2002; Karlsson *et al.*, 2004; Ding *et al.*, 2014), we next wanted to explore the relationship between EHD2 and caveolin-1 in primary adipocytes differentiated in vivo. Optical sectioning by confocal microscopy demonstrated that EHD2 was localized to the same structures as both caveolin-1 and cavin1, presumably caveolae, in the plasma membrane region of primary human adipocytes (Figure 5, A and B). Colocalization of these proteins was illustrated by plotting the fluorescence intensity profile of EHD2 (green) and caveolin-1/cavin1 (red) along a line drawn in the membrane-close region (Figure 5, A and B, line shown in insert, intensity plot in bottom panel).

Adrenergic stimulation induces accumulation of phosphorylated perilipin-1 and EHD2 at surface-associated lipid droplets

Next, we further examined the localization of EHD2 under insulin- and catecholamine-stimulated conditions. ISO, but not insulin, caused an accumulation of EHD2 at structures close to the plasma membrane, which resembled small lipid droplets (Figure 6A, top panel, EHD2 detected with antibody, shown in green). ISO also increased the signal of phosphorylated perilipin-1 (pS522) that was concentrated at the same structures as EHD2 (Figure 6A, second panel, perilipin-1 [pS522], shown as inverted gray). A similar distribution of EHD2 and phosphorylated perilipin-1 was also observed in EHD2 wild type (WT)-overexpressing cells (Figure 6A, bottom two panels, EHD2 detected with GFP, shown in green; perilipin-1 [pS522] shown as inverted gray). Interestingly, overexpression of EHD2 WT resulted

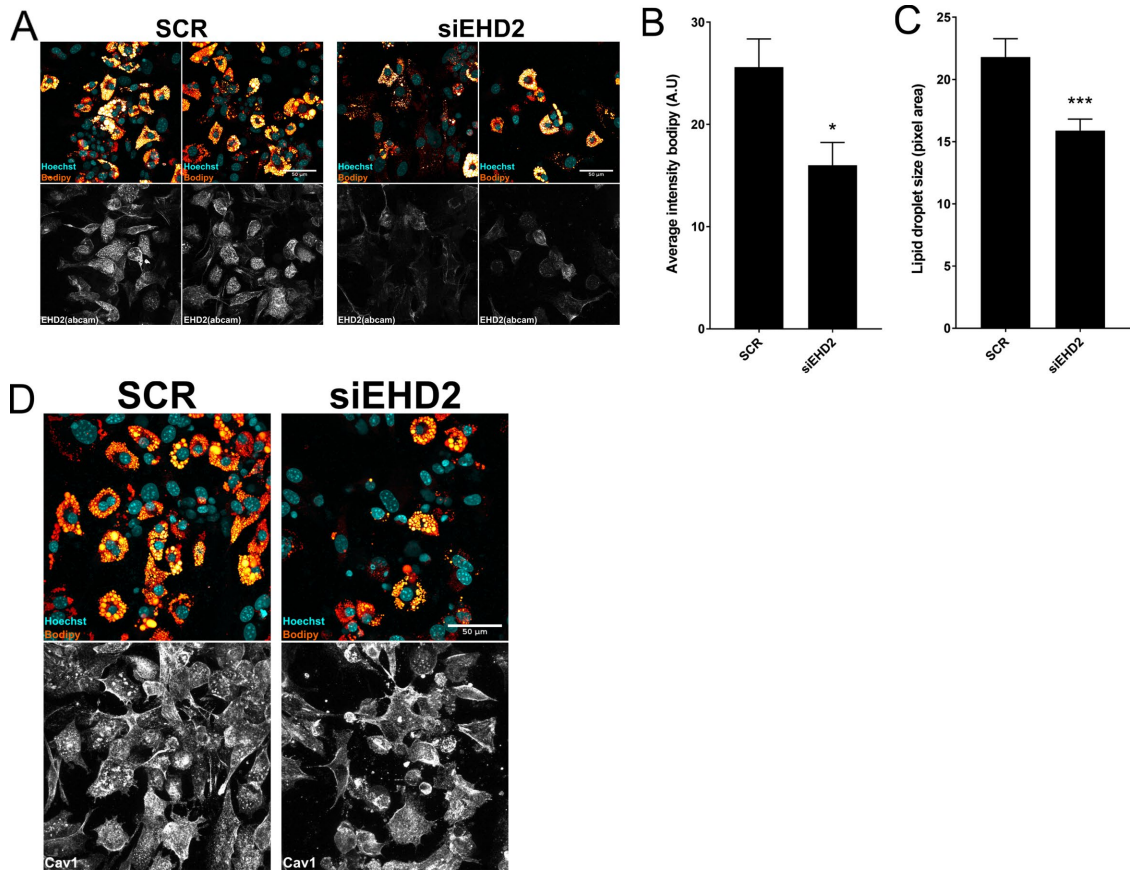

FIGURE 3: (A) Representative immunofluorescence images of 3T3-L1 cells: control (SCR, left panels) or EHD2-silenced (siEHD2, right panels), stained for nuclei (Hoechst, blue signal), neutral lipids (BODIPY, yellow signal), and EHD2 (gray scale). Scale bar = 50 µm. (B) Average intensity in arbitrary units (AU) of neutral lipids (BODIPY) in control (SCR) and EHD2-silenced (siEHD2) cells. (C) Quantification of lipid droplet size (relative size expressed as pixel area) in control (SCR) or EHD2-silenced (siEHD2) cells. Data are in presented as mean ± SEM.*$p < 0.05$, ***$p < 0.001$. (D) Representative immunofluorescence images of 3T3-L1 cells: control (SCR, left panels) or EHD2-silenced (siEHD2, right panels) that were stained for nuclei (Hoechst, blue signal), neutral lipids (BODIPY, yellow signal), and caveolin-1. Scale bar = 50 µm.

in a stronger perilipin-1 (p522) signal both in nonstimulated and ISO-stimulated cells compared with nontransfected cells (Figure 6A, panels showing the inverted gray). In a separate experiment using neutral lipid stain (BODIPY), we could confirm the presence of surface-associated lipid droplets (Supplemental Figure S3A). These lipid droplets were costained with perilipin-1 pS522 in the ISO-stimulated state. Note that these small lipid droplets are distinct from the main lipid droplet that was illustrated in Figure 5. Owing to technical limitations, it was not possible to examine whether EHD2, or perilipin-1, was also associated with the main lipid droplet.

To further verify the observation made by microscopy, primary human adipocytes were transduced with EHD2-encoding adenovirus and analyzed by Western blotting. EHD2 overexpression increased the level of ATGL and increased both basal and ISO-stimulated perilipin-1 pS522 (Figure 6B). EHD2 expression also induced the phosphorylation HSL pS563, shown in Figure 6C, bottom panel (not quantified due to low basal level).

Taken together, we demonstrate that EHD2 is located at caveolae (Figure 5) close to surface-associated lipid droplets in primary human adipocytes. These lipid droplets represent domains that have never been characterized in detail before. Further, the data suggest that an increased EHD2 level drives a lipolytic phenotype, shown as increased phosphorylation of both perilipin-1 and HSL and increased ATGL level. The fact that the surface-associated lipid droplets stained positive for perilipin-1 pS522 indeed suggests that they participate in lipolytic events.

The state of EHD2 oligomerization affects the distribution of caveolin-1

To act as a caveola stabilizer, ATP-bound EHD2 associates to the plasma membrane, followed by EHD2 oligomerization, which stabilizes the curvature of the caveolae neck (Hoernke *et al.*, 2017). To examine whether the membrane-binding, oligomerization, and ATPase activity affects EHD2 localization, we overexpressed EHD2 WT and the EHD2 mutants I157Q (having an intrinsically enhanced ATP hydrolysis activity leading to prolonged caveolar localization and stabilization) (Daumke *et al.*, 2007; Stoeber *et al.*, 2012) and F122A (which does not oligomerize) (Daumke *et al.*, 2007; Moren *et al.*, 2012), together with RFP-tagged caveolin-1 in primary human adipocytes. Imaging demonstrated that EHD2 WT and I157Q bound to the plasma membrane and localized together with caveolin-1 (illustrated in Figure 6C, EHD2 green signal, caveolin-1 red signal; top panel shows entire cell, and bottom panels show zoomed region of the cell). Overexpressed caveolin-1, in addition to exhibiting a strong membrane-associated signal, localized around lipid droplets that were identified by LipidTOX staining (Figure 6C, caveolin-1 red signal, LipidTOX gray signal). This localization could presumably

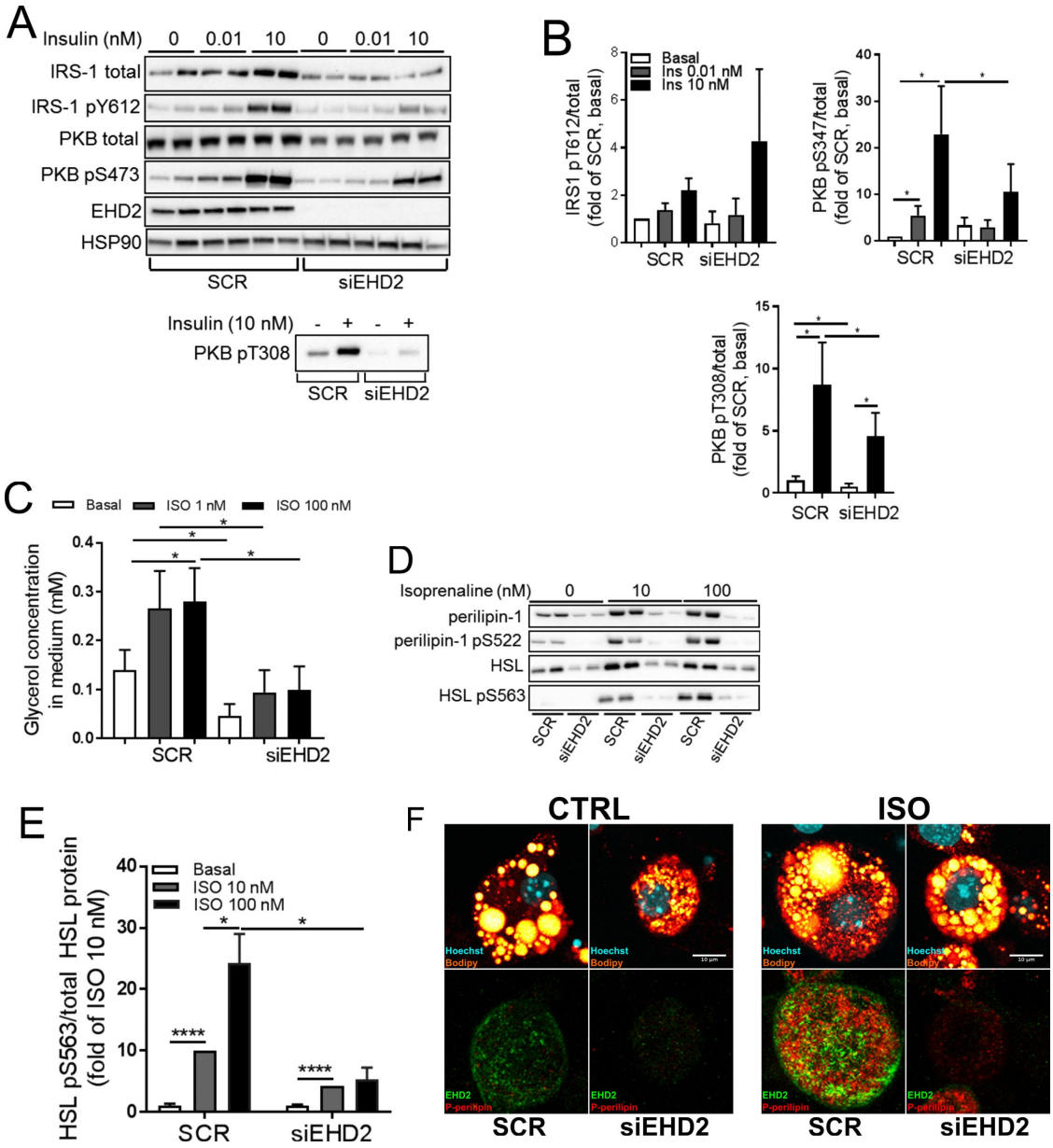

FIGURE 4: (A) Seventy-two hours after EHD2 gene silencing (scrambled [SCR] or siEHD2), 3T3-L1 cells were nonstimulated or stimulated with insulin (0.01, 0.1, or 10 nM) for 30 min followed by Western blot analysis to detect total and phosphorylated protein levels of IRS-1 (pY612), PKB (pS473), and EHD2. HSP90 used as a loading control. Levels of PKB (pT308) are shown in the bottom panel. Representative blots from $n = 34$ independent experiments. Quantifications of Western blot analysis in A are shown in B. Seventy-two hours after gene silencing (SCR or siEHD2-treated), 3T3-L1 cells were either nonstimulated or stimulated with ISO (10 or 100 nM) for 30 min; glycerol concentration in medium (mM) is shown in C, and Western blot analysis for detection of total and phosphorylated protein levels of HSL (pS563) and perilipin-1 (pS522) are shown in D. Representative blots from $n = 4$ independent experiments. (E) Quantification of HSL in D, expressed as HSL pS563/total HSL, $n = 4$ independent experiments; each sample was run in duplicate. Data in B, C, and E are shown as mean ± SD. *$p < 0.05$, ****$p < 0.0001$. (F) Representative immunofluorescence images of 3T3-L1 cells scrambled (SCR) or EHD2-silenced (siEHD2) that were either nontreated (CTRL, left panel) or ISO-treated (100 nM, right panel) for 30 min. After treatment, cells were fixed and stained for nuclei (Hoechst, blue signal), neutral lipids (BODIPY, yellow signal), EHD2 (green signal), and perilipin-1 pS522 (red signal). Scale bar = 10 μm.

mirror a normal function of caveolin-1 at the lipid droplet coats, a phenotype that is then enhanced when caveolin-1 is overexpressed. Disruption of the oligomerization of EHD2 by the F122A mutation resulted in a dispersed signal of caveolin-1 around the lipid droplets (Figure 6C, far right panel). Altogether, this suggests that the state of EHD2 oligomerization affects the lipid droplet-associated distribution of caveolin-1.

Lipolytic activity at surface-associated lipid droplets is dependent on ATP hydrolysis

Next, the distributions of the EHD2 mutants were also analyzed in the ISO-stimulated state. Because the I157Q mutant, having fast ATP hydrolysis, displayed a similar distribution as EHD2 WT (Figure 6C), we also included the EHD2 T94A mutant, exhibiting slow ATP hydrolysis, for comparison. The samples were costained

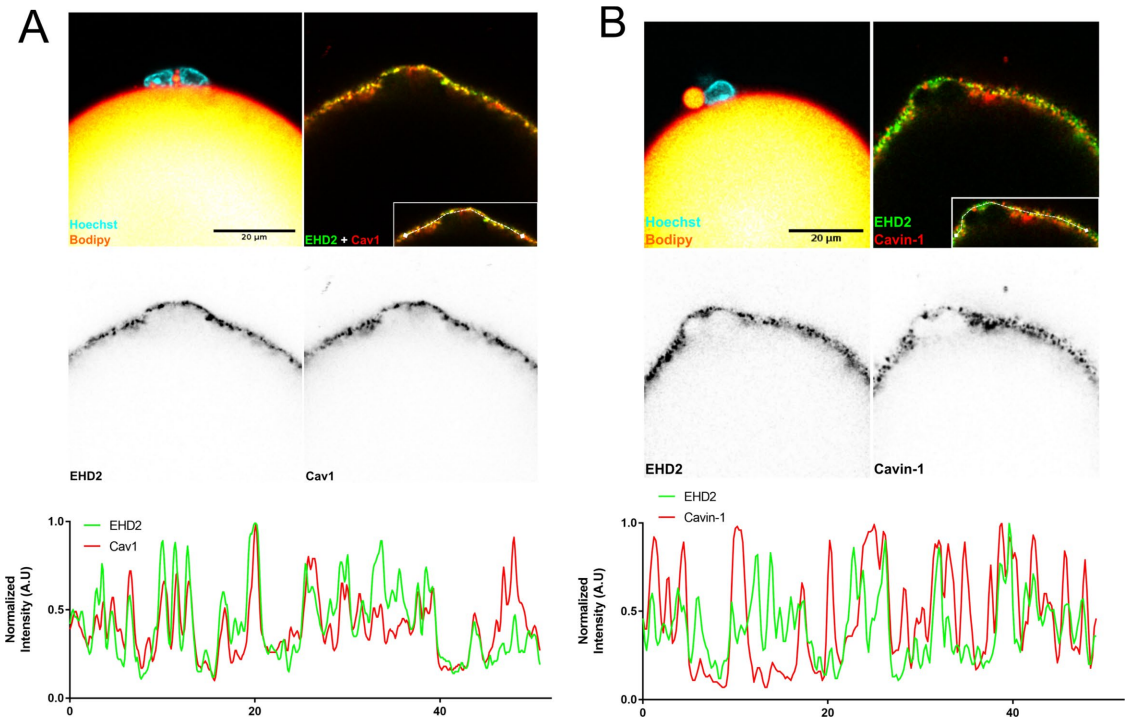

FIGURE 5: (A) Confocal microscopy images of primary human adipocytes that were fixed and stained for nuclei (Hoechst, blue signal) and neutral lipids (BODIPY, yellow); merged image is shown in the top left panel. The same cells were also stained with EHD2 (bottom left panel) and caveolin-1 (bottom right panel). Note that, the top right panel shows the merged image of EHD2 (green) and caveolin-1 (Cav1, red), and colocalization appears as a yellow signal. The insert shows a line drawn along the plasma membrane, and the fluorescence intensity profile (AU) is shown at the bottom to illustrate colocalization. Green represents EHD2, and red represents caveolin-1 (Cav1). (B) Same as in A but costained against cavin1 (Cavin-1, red). Scale bar = 20 µm.

with antibodies against either perilipin-1 pS522 or aquaporin 7 (AQP7), an adipocyte-specific glycerol transporter that facilitates glycerol release from adipocytes, here used as a marker to examine whether the lipid droplets potentially were associated with glycerol release (Kishida *et al.*, 2000). The I157Q mutant exhibited a phenotype similar to WT (Figure 7A, third panel), whereas cells expressing the T94A mutant displayed a more dispersed EHD2 signal and fewer lipid droplets, compared with WT (Figure 7A, far right panel). As shown in Figure 6A, ISO increased the signal of perilipin-1 pS522 at EHD2-positive surface lipid droplets in cells expressing EHD2 WT, I157Q, or T94A mutant (Figure 7A, top panel, quantification of perilipin-1 pS522 is shown in Figure 7B). The perilipin-1 pS522 signal was lower in cells expressing either I157Q or T94A mutant compared with WT (Figure 7B). The AQP7 signal was clustered at the same structures as perilipin-1 pS522 in all samples (Figure 7A, bottom panel). The presence of AQP7 at these lipid droplets suggests that they are associated with glycerol transport from the cell. Note that, in Figure 7, the signal levels have been optimized for visibility. In Supplemental Figure S4, the images of EHD2, AQP7, and perilipin-1 pS522 are shown as captured when using the same settings, demonstrating the relative differences in signal intensity among the EHD2 variants. Possibly, these differences among some of the EHD2 variants could reflect lower expression levels or distinct cellular localization. Supplemental Figure S4 also includes the EHD2 mutants T72A (no ATP binding), F122A (no oligomerization), and K328D (impaired membrane association), which exhibited lower expression or shifted localization and lower perilipin-1 pS522 activation at caveolae and lipid droplets at the membrane surface.

Regardless of the cause behind the different intensity levels of the EHD2 variants, these data together support that EHD2 drives a phenotype characterized by an accumulation of small lipid droplets that stain positive for both AQP7 and phosphorylated perilipin-1.

Overexpression of EHD2 and caveolin-1 impairs PPAR response element activity

Next, we wanted to examine potential mechanisms behind the EHD2-mediated effect on adipocyte maturation, which we observed earlier (data shown in Figure 2), a process tightly regulated by several transcription factors. EHD2 has previously been reported to accumulate in the nuclear fraction and to function as a transcriptional corepressor in nonadipocyte cell lines (Pekar *et al.*, 2012) and to connect caveolae disassembly with transcriptional activity (Torrino *et al.*, 2018). Here, by confocal microscopy, we found a punctuated distribution of EHD2 in the perinuclear region, but no significant amount was detected inside the nucleus (Figure 8A). Possibly, EHD2 could influence transcriptional activity indirectly by regulating the influx of fatty acids via caveolae, the former acting as ligands for nuclear receptors. To test this, primary human adipocytes were cotransfected with EHD2 variants and a PPAR response element (PPRE)-luciferase reporter, reflecting PPARγ activity. EHD2 WT overexpression decreased the PPRE activity with ~50% compared with control (Figure 8B). The EHD2 I157Q variant, which has prolonged caveolar localization, caused an even further reduction (~75%) of PPRE activity compared with control (Figure 8C). Thus, stabilization of EHD2 oligomers seemed to impair PPARγ activity in primary adipocytes. The T94A variant, which is unable to stabilize caveolae to the same extent as EHD2

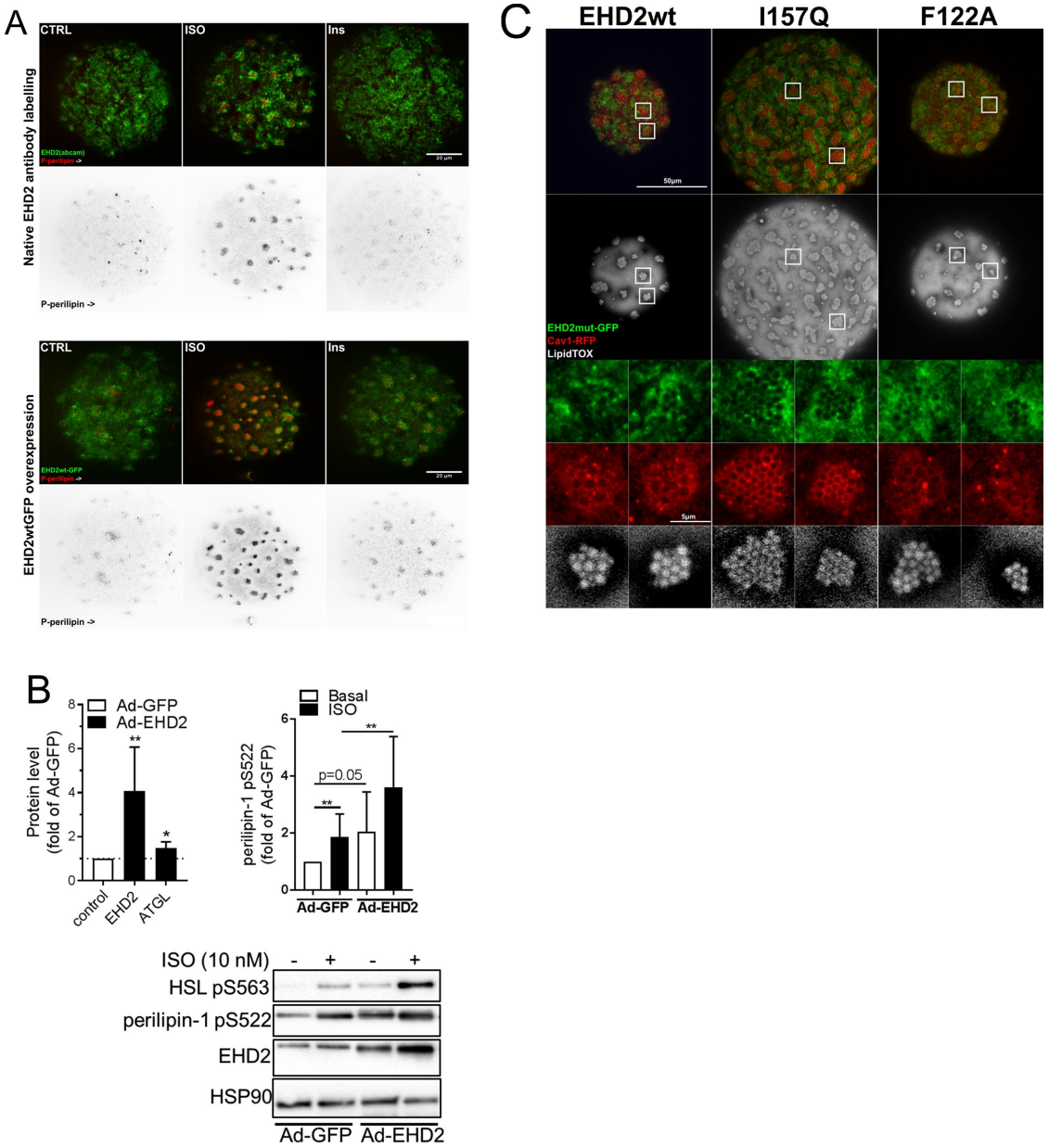

FIGURE 6: (A) The top panel illustrates native EDH2 antibody labeling of primary human adipocytes that were either nontreated (CTRL) or treated with ISO (100 nM, 30 min) or insulin (Ins, 100 nM, 30 min) prior to fixation. Staining with antibodies against EHD2 (green signal) and perilipin-1 pS522 (red signal). The perilipin-1 pS522 (P-perilipin) signal is also displayed in inverted gray scale below each image. The same conditions in EHD2WT-GFP overexpressing cells are shown in the bottom panel, where EHD2 was detected with GFP (green signal). Scale bar = 20 µm. (B) Protein expression assessed by Western blot in cell lysates from primary human adipocytes transduced with control (Ad-GFP) or Ad-EHD2 (Ad-EHD2WT) virus for 68–94 h, whereafter they were nontreated or treated with ISO (100 nM, 30 min). HSP90 was used for normalization. Data are expressed as fold expression compared with control (Ad-GFP) and presented as mean ± SD, $n = 5–6$ independent experiments. *$p < 0.05$, **$p < 0.01$. (C) Representative confocal microscopy images of primary human adipocytes expressing caveolin-1-RFP (Cav1-RFP) and either EHD2 WT (nonstimulated) or EHD2 mutants with single amino acid substitutions (all EHD2 constructs were GFP-tagged). Cells were also stained with LipidTOX to detected lipid droplets prior to imaging. The two top panels illustrate the distribution at the single cell level, scale bar = 50 µm. Magnified regions (white squares) showing distribution of EHD2 and caveolin-1 in lipid droplets in the surface proximal region are shown in the bottom panels, scale bar = 5 µm.

WT or I157Q, had a PPRE activity similar to that of the control (Figure 8C). Overexpression of caveolin-1 alone decreased PPRE activity with ~50%, similar to EHD2 WT (Figure 8C). Together, increased expression of either caveolin-1 or EHD2 seems sufficient to shift transcriptional activity.

DISCUSSION

In the present study, we have explored and confirmed a role of EHD2 for adipocyte function. We demonstrate that EHD2 is necessary for adipocyte maturation, triglyceride storage, and maintained cellular hormone sensitivity. We also show that EHD2 is located at

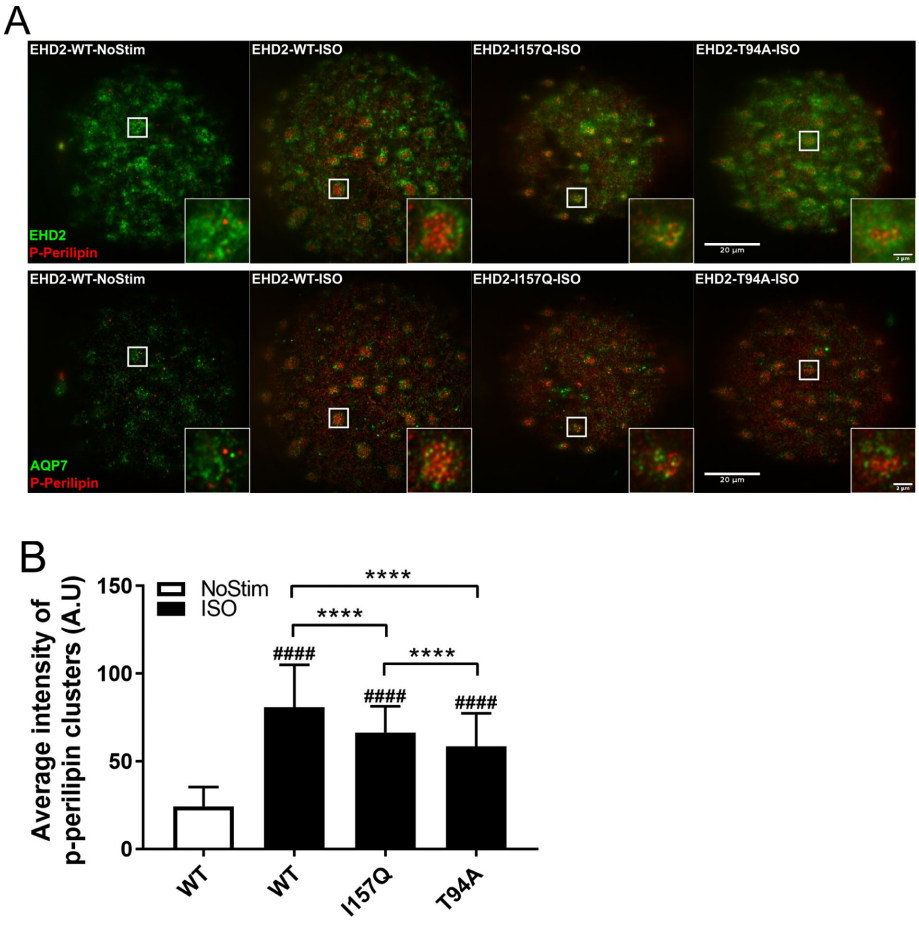

FIGURE 7: (A) Representative TIRF microscopy images of primary human adipocytes expressing EHD2 WT (nonstimulated) or EHD2 mutants (all stimulated with ISO 100 nM for 30 min prior fixation). In the top panel, the cells were stained with antibody against perilipin-1 pS522 (red), and EHD2 was detected by GFP signal (green). In the bottom panel, cells were costained against perilipin-1 pS522 (red) and AQP7 (green). Scale bar = 20 µm. Insets show zoom of lipid droplet structures for increased visibility. EHD2 and AQP7 are shown in green in each panel, and perilipin-1 pS522 is shown in red. Scale bar = 2 µm. (B) Fluorescence signal of perilipin-1 pS522 was quantified for each EHD2 mutant using an region of interest around each lipid cluster. Four clusters per cell and ~16 cells per EHD2 mutant were measured. ****$p < 0.0001$, ####$p < 0.0001$ significance levels compared with EHD2WT, nonstimulated (WT-NoStim).

caveolae in primary human adipocytes and provide the first characterization of surface-associated lipid droplets located close to EHD2. We provide several pieces of evidence that support these statements, as discussed below.

First, we found EHD2 to be up-regulated during adipose tissue expansion at a time point of significant adipocyte differentiation. Because the increased EHD2 level was detected in adipose tissue, and not isolated adipocytes, it is reasonable to believe this reflects an increased number of maturated adipocytes within the tissue. Second, we report a distinct increase of EHD2 expression that coincided with an increased expression of FAS and lipid accumulation in adipocytes differentiated in vitro. Third, EHD2-gene silencing decreased the expression of several transcriptional factors that are known as essential for adipogenesis (Farmer, 2006) and impaired the hormone response and lipid accumulation.

A couple of studies have previously mentioned EHD2 in the context of adipocyte differentiation (Bluher *et al.*, 2004; Molina *et al.*, 2009). By proteomic analysis, EHD2 was identified as one of several targets down-regulated in white adipose tissue from the adipose tissue-specific insulin receptor knock-out (FIRKO) mouse model (Bluher *et al.*, 2002, 2004). Since FIRKO mice have impaired glucose tolerance, severely altered adipocyte function, and reduced fat mass, EHD2 was proposed to play a role in adipocyte differentiation. Also, a relative increase of EHD2 mRNA expression during the later stage of adipocyte maturation was detected using a proteomic approach based on five-plex SILAC (Molina *et al.*, 2009). Both studies are in agreement with our findings, and the latter study seems to reflect changes during the maturation process of committed cells, which fits our data of increased EHD2 protein expression at the onset of lipid accumulation.

Although the molecular mechanisms involved in fatty acid uptake/release and triglyceride storage in adipocytes are not yet fully resolved (Thompson *et al.*, 2010), it is widely accepted that intact caveolae function is crucial for maintained lipid uptake (Razani *et al.*, 2002; Kim *et al.*, 2008; Ding *et al.*, 2014) as well as signal transduction (Karlsson *et al.*, 2004), even though the role of caveolin-1 for the latter has been reconsidered (Collins *et al.*, 2012). Indeed, in the past decade, a central role of cavin proteins for caveolae assembly and function has emerged (Bastiani *et al.*, 2009; Kovtun *et al.*, 2015). Here, we found EHD2 and caveolin-1 to increase simultaneously with the onset of lipid storage during adipocyte maturation in vitro and EHD2 to be localized to the same structures as both caveolin-1 and cavin1, most likely representing caveolae. Further, we show that in tissues from caveolin-1–deficient mice, the EHD2 expression was completely suppressed. On the basis of previous studies linking EHD2 to caveolae, we believe that EHD2 is necessary to sustain caveolar function in adipocytes, which is in line with previous reports in other cell systems (Moren *et al.*, 2012; Ludwig *et al.*, 2013; Shah *et al.*, 2014). The fact that we found EHD2-silencing to impair both hormonal response and lipid flux in cells during differentiation suggests that EHD2 is required for intact adipocyte function.

Primary adipocytes, aside from being fully differentiated, hold one large lipid droplet generated by esterification of exogenous fatty acids, which is in contrast to 3T3-L1 adipocytes that accumulate triglycerides in multiple lipid droplets mainly formed by de novo lipid synthesis. Whereas the biochemical steps of triglyceride synthesis and hydrolysis are well characterized, the exact subcellular sites for esterification and release of fatty acids and glycerol out of the cell are less described, as reviewed in Thompson *et al.* (2010). Possibly, fatty acids are accumulated in the caveolar membranes and are subsequently endocytosed for further metabolism. In human adipocytes, triglycerides were found to be synthesized in a subclass of caveolae (Ost *et al.*, 2005), which was also the site of uptake of exogenous fatty acids. Surprisingly, we identified a high spatial association of EHD2 and caveolin-1 close to

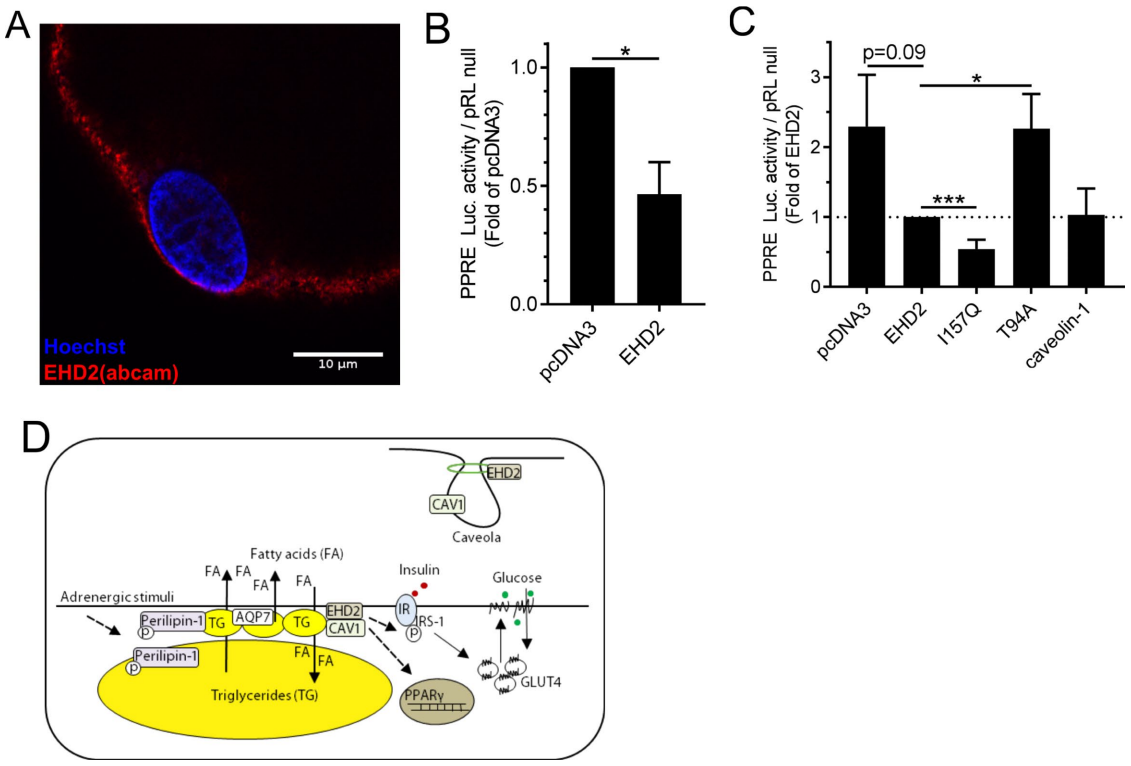

FIGURE 8: (A) Confocal cross-section of primary human adipocyte showing distribution of EHD2 stained with antibody (Abcam, red) and Hoechst (blue). Scale bar = 10 µm. (B, C) Levels of PPRE luciferase activity in response to overexpression of caveolin-1, EHD2, or EHD2 mutants with single amino acid substitutions. All PPRE activity levels were normalized to the levels of pRL null using a dual luciferase assay. In B, data are presented as fold of the PPRE luciferase activity in the pcDNA3-transduced control sample within each experiment, $n = 3$ independent experiments. Data are presented as mean ± SD. In C, the data are expressed as fold of the PPRE luciferase activity in the EHD2-transduced sample within each experiment. Data are presented as mean ± SD, $n = 3$–7 independent experiments/group. *$p < 0.05$, ***$p < 0.001$. (D) Graphic summary illustrating the localization of EHD2, together with caveolin-1, close to cell surface–associated lipid droplets that display lipolytic activity in primary human adipocytes. The dynamics of lipid transport across the cell membrane are dependent on EHD2, likely in a caveolae-dependent manner, which indirectly affects the transcriptional activity. Altogether, these data suggest that EHD2 plays a key role in maintaining adipocyte function.

surface-associated lipid droplets in primary human adipocytes. The presence of both AQP7 and phosphorylated perilipin-1 at these lipid droplets, the latter highly enriched in response to adrenergic stimulation, suggests that glycerol and fatty acid efflux could be mediated via caveolae. Possibly, these lipid domains are formed by lipid transfer from the large, central lipid droplet. In a recent study, it was stated that caveolin-1–deficient endothelial cells displayed impaired lipid droplet formation due to reduced lipolysis but not to altered triglyceride formation (Kuo *et al.*, 2018). The endothelial cell models seem to differ since caveolin-1 deficiency in adipocytes severely impairs the lipid storage capacity (Razani *et al.*, 2002). Still, the fact that we found overexpression of EHD2 to actually increase the lipolytic activity and the presence of surface-associated lipid droplets suggests that EHD2, possibly at the site of caveolae, could play a role in regulating lipolysis.

Perilipin-1, one of the first identified lipid droplet–associated protein (Greenberg *et al.*, 1991), was recently proposed to segregate into protein microdomains at the cell surface of human adipocytes (Hansen *et al.*, 2017). Still, no further description of the mechanistic function, or relation between these protein domains and caveolae or surface-associated lipid droplets, was provided. In an elegant study by Ariotti *et al.* (2012), lipolysis was associated with the formation of microlipid droplets (mLD) that were reformatted into large lipid droplets following insulin treatment (Ariotti *et al.*, 2012). Reesterification of fatty acids also increased the formation of cytosolic mLD that was subjected to lipolytic activity in Hashimoto *et al.* (2012). In agreement with previous reports, our data support the existence of specialized lipid droplets that are regulated by hormone action. Further, the fact that caveolin-1 and EHD2 previously were identified at intracellular lipid droplets by mass spectrometry (Blouin *et al.*, 2010) fits our data of EHD2 and caveolin-1 localization. Still, it is worth emphasizing that the narrow cytosolic space (100–150 nm thin) in primary adipocytes restricts the ability to resolve protein distribution between different pools of intracellular lipid droplets using light microscopy, and we have herein focused only on small lipid droplets close to the cell surface. Definitely, more detailed analyses at the ultrastructural level, including live cell imaging, are required to fully resolve the exact mechanisms by which EHD2 regulates caveolar function and lipid flux in primary adipocytes.

EHD2 has previously been described as a transcriptional corepressor (Pekar *et al.*, 2012) and also to connect caveolae disassembly with transcriptional regulation (Torrino *et al.*, 2018). Here, we found EHD2 overexpression to suppress the transcriptional activity of the nuclear receptor PPARγ. This was somewhat opposite the situation in differentiating 3T3-L1 cells, where EHD2 silencing

caused decreased PPARγ2 expression, which we interpreted to reflect halted maturation. Still, the two adipose models are distinct from each other with respect to the degree of maturation, and the results likely reflect different mechanisms. On the basis of our data, we propose that in primary adipocytes, EHD2 can affect PPARγ activity indirectly by altering uptake of fatty acids, which function as nuclear receptor ligands and thereby influence transcriptional activity (Lee *et al*., 2003).

On the basis of previous structural analysis of the mutated EHD2 variants (Daumke *et al*., 2007; Moren *et al*., 2012; Shah *et al*., 2014; Hoernke *et al*., 2017), we interpret their different capacities to suppress PPARγ activity to reflect their different impacts on the behavior/function of caveolae. For instance, overexpression of the I157Q variant, which stabilizes caveolae at the plasma membrane to a high degree, causes the strongest reduction in PPRE activity. In contrast, overexpression of the T94A variant, which previously was shown to stabilize caveolae to a lesser extent than I157Q or EHD2 WT, had no effect on PPRE activity. Other EHD2 mutants tested (T72A, F122A, and K328D) had similar effects on PPRE activity as EHD2 WT, but were not as consistent between the experiments (Supplemental Figure S4B). Independently of their various properties with respect to ATP hydrolysis, membrane, and ATP binding, almost all EHD2 mutants tested localized to the plasma membrane and to surface-associated lipid droplets in the human adipocytes. The only exception was the K328D mutant, which displayed a more pronounced association with lipid droplets that was difficult to interpret (Supplemental Figure S3B). Still, the fact that overexpression of caveolin-1 alone was sufficient to suppress PPARγ activity to the same extent as obtained with EHD2 WT supports the hypothesis that the EHD2-induced effect is dependent on caveolae function. PPARγ has been shown to directly interact with caveolin-1 in lipid raft fractions (Burgermeister *et al*., 2003, 2011), and we did observe PPARγ to be distributed not only in the nuclei but also in the plasma membrane (Supplemental Figure S3C), which potentially suggests a caveolae-dependent translocation of PPARγ.

In summary, in this report we demonstrate that EHD2 is up-regulated during adipocyte maturation in parallel with caveolin-1 expression, and that EHD2 silencing seems to halt differentiation and to affect insulin sensitivity and the ability to both form and hydrolyze lipids. Further, we show that EHD2 is located at caveolae, close to novel cell surface–associated lipid droplets structures that display lipolytic activity. Taking the results together, we suggest that the dynamics of lipid transport across the cell membrane are dependent on EHD2, likely in a caveolae-dependent manner (summarized in Figure 8D).

MATERIALS AND METHODS

Materials

3T3-L1 cells were purchased from the American Type Culture Collection, and the Quantifast SYBR Green RT-PCR kit was from Qiagen (Holden, Germany). The PPRE-X3-TK-Luc reporter plasmid was a kind gift from Bruce Spiegelman (Harvard University) (Addgene plasmid #1015), and the pcDNA3.3-eGFP plasmid was a kind gift from Derrick Rossi (Harvard University) (Addgene plasmid #26822). RFP-tagged caveolin-1, GFP-tagged EHD2 WT, and variants were kindly provided by Richard Lundmark (Umeå University, Sweden) and Oliver Daumke (MDC, Germany). Adenoviral vectors for GFP and EHD2 (GenBank accession numbers CU013410 and BC113161) were produced by Vector BioLabs (Philadelphia, PA). Heat shock protein (HSP) 90 antibody was from BD Transduction Laboratories (Franklin Lakes, NJ). FAS, caveolin-1, IRS-1 total and pT612, ACC, FABP4/ap2, ATGL, C/EBPα, PKB total and pS473, and HSL total and pS563 antibodies were from Cell Signaling Technologies (Danvers, MA). The anti–perilipin-1 antibodies were from Vala Science (San Diego, CA), and the antibodies against EHD2 (ab154784), AQP7, cavin1, and antibody conjugation kit were from Abcam (Cambridge, UK). The total HSL antibody was kindly provided by Cecilia Holm (Lund University). Fluorescence–conjugated (Alexa Fluor) secondary antibodies and BODIPY were purchased from Molecular Probe (Waltham, MA). Reagent for determination of glycerol content (F6428) was from Sigma-Aldrich (St. Louis, MO).

Human and animal studies

The human studies and animal procedures were approved by the local ethical committee. The human tissue was collected after written informed consent from the patients.

Preparation of primary adipocytes and adenoviral overexpression

Subcutaneous white adipose tissue was removed during reconstructive surgery, and primary adipocytes were isolated from the tissue using an established protocol (Rodbell, 1964). The patients, all female, were without known diabetes (type 1 or type 2) or thyroid gland dysfunction. In experiments using mouse adipocytes or adipose tissue, cells were isolated from epididymal fat pads from c57Bl/6J male mice (Taconic) or caveolin-1 KO mice (Sadegh *et al*., 2011). Isolated cells were suspended (20% [vol/vol]) in Krebs-Ringer Bicarbonate HEPES (KRBH) buffer, pH 7.4, containing 200 nM adenosine and 1% (wt/vol) bovine serum albumin (BSA). Cells used for adenoviral overexpression were suspended in DMEM with penicillin/streptomycin (100 U/ml and 100 µg/ml, respectively), 200 nM phenyl-isopropyl-adenosin (PIA), and 3.5% (wt/vol) BSA and cultured at 5% CO_2, 37°C for 72 h with EHD2 or control (GFP) virus. In the adenoviral overexpression experiments, 400 µl of isolated adipocytes per condition (Ad-GFP or Ad-EHD2) was cultured in 1100 µl of supplemented DMEM (described above). After virus incubation, the cells were washed in KRBH buffer, followed by stimulation according to the figures.

Cell culture and EHD2 silencing

3T3-L1 fibroblasts were cultured and differentiated as previously described (Hansson, 2017). In short, cells were cultured at subconfluence in DMEM containing 10% fetal calf serum (FCS) (vol/vol) and 1% penicillin/streptomycin (vol/vol) in an atmosphere with 5% CO_2 at 37°C. For differentiation, cells were incubated with DMEM containing 10% (vol/vol) FCS, penicillin/streptomycin (100 U/ml and 100 µg/ml, respectively), 0.5 mM 3-isobutyl-L-methylxanthine, 10 µg/ml insulin, and 1 µM dexamethasone for 72 h for 2 d postconfluence (designated day 0). Thereafter, cells were cultured in DMEM containing 10% (vol/vol) FCS and penicillin/streptomycin until day 11. EHD2 silencing was performed as previously described (Hansson, 2017) by electroporation at day 4 using siRNA targeting EHD2 (MSS281816) or scrambled siRNA (SCR) (negative control; #12935300; Invitrogen, Waltham, MA).

Glycerol release

To measure glycerol release, cells were washed in KRH medium with 3% BSA and treated with ISO as indicated in the figures for 1 h. Cell medium was subsequently removed for enzymatic determination of the glycerol content. In short, 100 µl free glycerol reagent was added to 30 µl sample. Absorbance at 540 nm was measured after incubating for ~15 min at room temperature. Each sample was analyzed in duplicate.

Confocal and TIRF imaging

Imaging was performed using a Nikon A1 plus confocal microscope with a 60× Apo DIC oil immersion objective with a NA of 1.40 (Nikon Instruments) and appropriate filter sets. Images were acquired with NIS-Elements, version: 4.50.02 (Laboratory Imaging). For TIRF imaging, we used a commercial TIRF system based on a Nikon Ti-E eclipse microscope equipped with a 100× Apo TIRF DIC oil immersion objective with a NA of 1.49 (Nikon Instruments), an iXon Ultra DU-897 EMCCD camera (Andor Technology), and four main laser lines: 405 (Cube, Coherent), 488 (Melles-Griot), 561 (Sapphire, Coherent), and 640 (Cube, Coherent) with corresponding filter sets. Images are usually acquired at a generous TIRF angle to allow imaging of protein stains related to lipid droplets, such as phosphoperilipin-1. Isolated cells were fixed using 4% paraformaldehyde and labeled with antibodies in a buffer containing 1% BSA, 1% goat serum, and 0.05% saponin 1–2 h per labeled antibody. For neutral lipid staining, BODPIY was used in conjunction with confocal imaging. TIRF microscopy was used to detect protein stain only. For imaging of adipocytes, we used previously described protocol (Wasserstrom *et al.*, 2018).

Western blot

Following incubations, cells were washed with KRH medium without BSA and subsequently lysed in a buffer containing 50 mM Tris-HCl, pH 7.5, 1 mM ethylene glycol tetraacetic acid, 1 mM EDTA, 0.27 M sucrose, 1% NP-40, and complete protease- and phosphatase-inhibitor cocktail (Roche, Basel, Switzerland). Lysates were centrifuged for 10 min at 13,000 × *g*, and protein concentrations were determined using the Bradford method. Samples were subjected to PAGE and electro-transfer to nitrocellulose membranes. Membranes were blocked with nonfat dry milk (10% [wt/vol]) and probed with the indicated antibodies. Detection was performed using horseradish peroxidase–conjugated secondary antibodies and enhanced chemiluminescence reagent. The signal was visualized using a Bio-Rad Image camera (Bio-Rad, Hercules, CA).

Plasmid transfection and luciferase activity assays

Adipocytes were transfected as previously described (Lizunov *et al.*, 2013). In short, isolated adipose cells were suspended (40% [vol/vol]) in DMEM supplemented with penicillin/streptomycin (100 U/ml and 100 µg/ml, respectively) and 200 nM PIA. Cells were electroporated using a square-wave pulse, 400 V, 12 ms, and one pulse (Harvard Apparatus, Holliston, MA) with plasmids as indicated (protein encoding plasmid:reporter:control at 20:10:1). After electroporation, the cells were transferred into DMEM with penicillin/streptomycin, PIA, and 3.5% (wt/vol) BSA and cultured for 20 h at 37°C in 5% CO2. Thereafter, the cells were lysed in Promega passive lysis buffer, and the lysates were centrifuged at 1000 × *g* for 10 min at 4°C to separate the protein lysate (infranatant) from the fat. Luciferase activity was measured in a Glomax luminometer (Promega) using the Dual Luciferase Reporter system (Promega).

Statistical analysis

Analysis was performed by one-way analysis of variance and multiple comparisons, or Student's *t* test when appropriate, using GraphPad Prism 6 (Graphpad Software) software. Significance was determined according to $*p < 0.05$, $**p < 0.01$, $***p < 0.001$, and $****p < 0.0001$.

ACKNOWLEDGMENTS

We thank Maria Lindahl for excellent technical support. We also thank the Lund University Bioimaging Center (LBIC) for assistance with sample preparation. This work was financially supported by the Swedish Research Council (2013-3542 and Strategic Research Area Exodiab, Dnr 2009-1039), the Swedish Foundation for Strategic Research Dnr IRC15-0067, Novo Nordisk (NNF17OC0027054), the Swedish Diabetes Foundation, The Crafoord Foundation, the Albert Påhlsson Foundation, and the Royal Physiographic Society in Lund.

REFERENCES

Aboulaich N, Vainonen JP, Stralfors P, Vener AV (2004). Vectorial proteomics reveal targeting, phosphorylation and specific fragmentation of polymerase I and transcript release factor (PTRF) at the surface of caveolae in human adipocytes. Biochem J 383, 237–248.

Acosta JR, Douagi I, Andersson DP, Backdahl J, Ryden M, Arner P, Laurencikiene J (2016). Increased fat cell size: a major phenotype of subcutaneous white adipose tissue in non-obese individuals with type 2 diabetes. Diabetologia 59, 560–570.

Ariotti N, Murphy S, Hamilton NA, Wu L, Green K, Schieber NL, Li P, Martin S, Parton RG (2012). Postlipolytic insulin-dependent remodeling of micro lipid droplets in adipocytes. Mol Biol Cell 23, 1826–1837.

Bastiani M, Liu L, Hill MM, Jedrychowski MP, Nixon SJ, Lo HP, Abankwa D, Luetterforst R, Fernandez-Rojo M, Breen MR, *et al.* (2009). MURC/Cavin-4 and cavin family members form tissue-specific caveolar complexes. J Cell Biol 185, 1259–1273.

Blouin CM, Le Lay S, Eberl A, Kofeler HC, Guerrera IC, Klein C, Le Liepvre X, Lasnier F, Bourron O, Gautier JF, *et al.* (2010). Lipid droplet analysis in caveolin-deficient adipocytes: alterations in surface phospholipid composition and maturation defects. J Lipid Res 51, 945–956.

Bluher M, Michael MD, Peroni OD, Ueki K, Carter N, Kahn BB, Kahn CR (2002). Adipose tissue selective insulin receptor knockout protects against obesity and obesity-related glucose intolerance. Dev Cell 3, 25–38.

Bluher M, Patti ME, Gesta S, Kahn BB, Kahn CR (2004). Intrinsic heterogeneity in adipose tissue of fat-specific insulin receptor knock-out mice is associated with differences in patterns of gene expression. J Biol Chem 279, 31891–31901.

Burgermeister E, Friedrich T, Hitkova I, Regel I, Einwachter H, Zimmermann W, Rocken C, Perren A, Wright MB, Schmid RM, *et al.* (2011). The Ras inhibitors caveolin-1 and docking protein 1 activate peroxisome proliferator-activated receptor gamma through spatial relocalization at helix 7 of its ligand-binding domain. Mol Cell Biol 31, 3497–3510.

Burgermeister E, Tencer L, Liscovitch M (2003). Peroxisome proliferator-activated receptor-gamma upregulates caveolin-1 and caveolin-2 expression in human carcinoma cells. Oncogene 22, 3888–3900.

Cohen AW, Razani B, Wang XB, Combs TP, Williams TM, Scherer PE, Lisanti MP (2003). Caveolin-1-deficient mice show insulin resistance and defective insulin receptor protein expression in adipose tissue. Am J Physiol 285, C222–C235.

Collins BM, Davis MJ, Hancock JF, Parton RG (2012). Structure-based reassessment of the caveolin signaling model: do caveolae regulate signaling through caveolin-protein interactions? Dev Cell 23, 11–20.

Daumke O, Lundmark R, Vallis Y, Martens S, Butler PJ, McMahon HT (2007). Architectural and mechanistic insights into an EHD ATPase involved in membrane remodelling. Nature 449, 923–927.

Ding SY, Lee MJ, Summer R, Liu L, Fried SK, Pilch PF (2014). Pleiotropic effects of cavin-1 deficiency on lipid metabolism. J Biol Chem 289, 8473–8483.

Farmer SR (2006). Transcriptional control of adipocyte formation. Cell Metabolism 4, 263–273.

Fielding CJ, Fielding PE (2001). Caveolae and intracellular trafficking of cholesterol. Adv Drug Deliv Rev 49, 251–264.

Fu Y, Luo N, Klein RL, Garvey WT (2005). Adiponectin promotes adipocyte differentiation, insulin sensitivity, and lipid accumulation. J Lipid Res 46, 1369–1379.

Greenberg AS, Egan JJ, Wek SA, Garty NB, Blanchette-Mackie EJ, Londos C (1991). Perilipin, a major hormonally regulated adipocyte-specific phosphoprotein associated with the periphery of lipid storage droplets. J Biol Chem 266, 11341–11346.

Grunberg JR, Hammarstedt A, Hedjazifar S, Smith U (2014). The novel secreted adipokine WNT1-inducible signaling pathway protein 2 (WISP2) is a mesenchymal cell activator of canonical WNT. J Biol Chem 289, 6899–6907.

Guilherme A, Soriano NA, Bose S, Holik J, Bose A, Pomerleau DP, Furcinitti P, Leszyk J, Corvera S, Czech MP (2004). EHD2 and the novel EH domain binding protein EHBP1 couple endocytosis to the actin cytoskeleton. J Biol Chem 279, 10593–10605.

Gustavsson J, Parpal S, Karlsson M, Ramsing C, Thorn H, Borg M, Lindroth M, Peterson KH, Magnusson KE, Stralfors P (1999). Localization of the insulin receptor in caveolae of adipocyte plasma membrane. FASEB J 13, 1961–1971.
Hansen JS, de Mare S, Jones HA, Goransson O, Lindkvist-Petersson K (2017). Visualization of lipid directed dynamics of perilipin 1 in human primary adipocytes. Sci Rep 7, 15011.
Hansson B, Rippe C, Kotowska D, Wasserstrom S, Säll J, Göransson O, Swärd K, Stenkula KG. (2017). Rosiglitazone drives cavin-2/SDPR expression in adipocytes in a CEBPα-dependent manner. PloS One 12, e0173412.
Hansson B, Wasserstrom S, Moren B, Periwal V, Vikman P, Cushman S, Goransson O, Storm P, Stenkula K (2018). Intact glucose uptake despite deteriorating signaling in adipocytes with high-fat feeding. J Mol Endocrinol 60, 199–211.
Hashimoto T, Segawa H, Okuno M, Kano H, Hamaguchi HO, Haraguchi T, Hiraoka Y, Hasui S, Yamaguchi T, Hirose F, *et al.* (2012). Active involvement of micro-lipid droplets and lipid-droplet-associated proteins in hormone-stimulated lipolysis in adipocytes. J Cell Sci 125, 6127–6136.
Hoernke M, Mohan J, Larsson E, Blomberg J, Kahra D, Westenhoff S, Schwieger C, Lundmark R (2017). EHD2 restrains dynamics of caveolae by an ATP-dependent, membrane-bound, open conformation. Proc Natl Acad Sci USA 114, E4360–E4369.
Karlsson M, Thorn H, Danielsson A, Stenkula KG, Ost A, Gustavsson J, Nystrom FH, Stralfors P (2004). Colocalization of insulin receptor and insulin receptor substrate-1 to caveolae in primary human adipocytes. Cholesterol depletion blocks insulin signalling for metabolic and mitogenic control. Eur J Biochem 271, 2471–2479.
Kim CA, Delepine M, Boutet E, El Mourabit H, Le Lay S, Meier M, Nemani M, Bridel E, Leite CC, Bertola DR, *et al.* (2008). Association of a homozygous nonsense caveolin-1 mutation with Berardinelli-Seip congenital lipodystrophy. J Clin Endocrinol Metab 93, 1129–1134.
Kishida K, Kuriyama H, Funahashi T, Shimomura I, Kihara S, Ouchi N, Nishida M, Nishizawa H, Matsuda M, Takahashi M, *et al.* (2000). Aquaporin adipose, a putative glycerol channel in adipocytes. J Biol Chem 275, 20896–20902.
Kovtun O, Tillu VA, Ariotti N, Parton RG, Collins BM (2015). Cavin family proteins and the assembly of caveolae. J Cell Sci 128, 1269–1278.
Kuo A, Lee MY, Yang K, Gross RW, Sessa WC (2018). Caveolin-1 regulates lipid droplet metabolism in endothelial cells via autocrine prostacyclin-stimulated, cAMP-mediated lipolysis. J Biol Chem 293, 973–983.
Lee CH, Olson P, Evans RM (2003). Minireview: lipid metabolism, metabolic diseases, and peroxisome proliferator-activated receptors. Endocrinology 144, 2201–2207.
Li Y, Periwal V, Cushman SW, Stenkula KG (2016). Adipose cell hypertrophy precedes the appearance of small adipocytes by 3 days in C57BL/6 mouse upon changing to a high fat diet. Adipocyte 5, 81–87.
Lizunov VA, Lee JP, Skarulis MC, Zimmerberg J, Cushman SW, Stenkula KG (2013). Impaired tethering and fusion of GLUT4 vesicles in insulin-resistant human adipose cells. Diabetes 62, 3114–3119.
Ludwig A, Howard G, Mendoza-Topaz C, Deerinck T, Mackey M, Sandin S, Ellisman MH, Nichols BJ (2013). Molecular composition and ultrastructure of the caveolar coat complex. PLoS Biol 11, e1001640.
McLaughlin T, Lamendola C, Coghlan N, Liu TC, Lerner K, Sherman A, Cushman SW (2014). Subcutaneous adipose cell size and distribution: relationship to insulin resistance and body fat. Obesity (Silver Spring) 22, 673–680.
McLaughlin T, Sherman A, Tsao P, Gonzalez O, Yee G, Lamendola C, Reaven GM, Cushman SW (2007). Enhanced proportion of small adipose cells in insulin-resistant vs insulin-sensitive obese individuals implicates impaired adipogenesis. Diabetologia 50, 1707–1715.
Meshulam T, Simard JR, Wharton J, Hamilton JA, Pilch PF (2006). Role of caveolin-1 and cholesterol in transmembrane fatty acid movement. Biochemistry 45, 2882–2893.
Molina H, Yang Y, Ruch T, Kim JW, Mortensen P, Otto T, Nalli A, Tang QQ, Lane MD, Chaerkady R, *et al.* (2009). Temporal profiling of the adipocyte proteome during differentiation using a five-plex SILAC based strategy. J Proteome Res 8, 48–58.
Moren B, Shah C, Howes MT, Schieber NL, McMahon HT, Parton RG, Daumke O, Lundmark R (2012). EHD2 regulates caveolar dynamics via ATP-driven targeting and oligomerization. Mol Biol Cell 23, 1316–1329.
Naslavsky N, Boehm M, Backlund PS Jr, Caplan S (2004). Rabenosyn-5 and EHD1 interact and sequentially regulate protein recycling to the plasma membrane. Mol Biol Cell 15, 2410–2422.
Ost A, Ortegren U, Gustavsson J, Nystrom FH, Stralfors P (2005). Triacylglycerol is synthesized in a specific subclass of caveolae in primary adipocytes. J Biol Chem 280, 5–8.
Park SY, Ha BG, Choi GH, Ryu J, Kim B, Jung CY, Lee W (2004). EHD2 interacts with the insulin-responsive glucose transporter (GLUT4) in rat adipocytes and may participate in insulin-induced GLUT4 recruitment. Biochemistry 43, 7552–7562.
Parton RG, del Pozo MA (2013). Caveolae as plasma membrane sensors, protectors and organizers. Nat Rev Mol Cell Biol 14, 98–112.
Pekar O, Benjamin S, Weidberg H, Smaldone S, Ramirez F, Horowitz M (2012). EHD2 shuttles to the nucleus and represses transcription. Biochem J 444, 383–394.
Razani B, Combs TP, Wang XB, Frank PG, Park DS, Russell RG, Li M, Tang B, Jelicks LA, Scherer PE, *et al.* (2002). Caveolin-1-deficient mice are lean, resistant to diet-induced obesity, and show hypertriglyceridemia with adipocyte abnormalities. J Biol Chem 277, 8635–8647.
Rodbell M (1964). Metabolism of isolated fat cells. i. effects of hormones on glucose metabolism and lipolysis. J Biol Chem 239, 375–380.
Sadegh MK, Ekman M, Rippe C, Sundler F, Wierup N, Mori M, Uvelius B, Sward K (2011). Biomechanical properties and innervation of the female caveolin-1-deficient detrusor. Br J Pharmacol 162, 1156–1170.
Salans LB, Knittle JL, Hirsch J (1968). The role of adipose cell size and adipose tissue insulin sensitivity in the carbohydrate intolerance of human obesity. J Clin Invest 47, 153–165.
Schinner S, Scherbaum WA, Bornstein SR, Barthel A (2005). Molecular mechanisms of insulin resistance. Diabet Med 22, 674–682.
Shah C, Hegde BG, Moren B, Behrmann E, Mielke T, Moenke G, Spahn CM, Lundmark R, Daumke O, Langen R (2014). Structural insights into membrane interaction and caveolar targeting of dynamin-like EHD2. Structure 22, 409–420.
Stoeber M, Stoeck IK, Hanni C, Bleck CK, Balistreri G, Helenius A (2012). Oligomers of the ATPase EHD2 confine caveolae to the plasma membrane through association with actin. EMBO J 31, 2350–2364.
Thompson BR, Lobo S, Bernlohr DA (2010). Fatty acid flux in adipocytes: the in's and out's of fat cell lipid trafficking. Mol Cell Endocrinol 318, 24–33.
Torrino S, Shen WW, Blouin CM, Mani SK, Viaris de Lesegno C, Bost P, Grassart A, Koster D, Valades-Cruz CA, Chambon V, *et al.* (2018). EHD2 is a mechanotransducer connecting caveolae dynamics with gene transcription. J Cell Biol 217, 4092–4105.
Wasserstrom S, Moren B, Stenkula KG (2018). Total internal reflection fluorescence microscopy to study GLUT4 trafficking. Methods Mol Biol 1713, 151–159.